Structural and magnetic properties of RFe_2D_x deuterides (R = Zr, Y and $x \geq 3.5$) studied by means of neutron diffraction and ^{57}Fe Mössbauer spectroscopy

2005 J. Phys.: Condens. Matter 17 893

(http://iopscience.iop.org/0953-8984/17/6/009)

INSTITUTE OF PHYSICS PUBLISHING JOURNAL OF PHYSICS: CONDENSED MATTER

J. Phys.: Condens. Matter **17** (2005) 893–908 doi:10.1088/0953-8984/17/6/009

Structural and magnetic properties of RFe_2D_x deuterides (R = Zr, Y and $x \geqslant 3.5$) studied by means of neutron diffraction and ^{57}Fe Mössbauer spectroscopy

G Wiesinger[1], V Paul-Boncour[2,4], S M Filipek[3], Ch Reichl[1], I Marchuk[3] and A Percheron-Guégan[2]

[1] Institute for Solid State Physics, TU Wien, Wiedner Hauptstrasse 8, A-1040 Vienna, Austria
[2] Laboratoire de Chimie Métallurgique des Terres Rares, CNRS, ISCSA, 2-8 rue Henri Dunant, F-94320 Thiais, France
[3] Institute of Physical Chemistry of the Polish Academy of Science, 01-224 Warsaw, Poland

E-mail: paulbon@glvt-cnrs.fr

Received 12 July 2004, in final form 4 January 2005
Published 28 January 2005
Online at stacks.iop.org/JPhysCM/17/893

Abstract

The structure of $YFe_2D_{3.5}$ at 290 K has been refined in a monoclinic superstructure using synchrotron radiation and neutron diffraction experiments. The evolution of the ^{57}Fe Mössbauer spectra versus temperature for $ZrFe_2D_x$ and YFe_2D_x deuterides with large deuterium content ($3.5 \leqslant x \leqslant 5$) has been studied. For $x = 3.5$ both $ZrFe_2D_x$ and YFe_2D_x show an increase of the Fe magnetization compared to the parent intermetallic compound, related to the increase of the cell volume. For YFe_2D_x the Fe moment decreases to complete disappearance as x increases from 3.5 to 5 due to the stronger influence of the Fe–D bonding compared to the volume increase. The evolution of the isomer shift can be attributed to an almost pure volumetric effect in the case of the YFe_2 deuterides, whereas for $ZrFe_2D_{3.5}$ additional D–Fe charge transfer has to be taken into account.

1. Introduction

During the last few decades hydrogen absorption and its influence on the structural, magnetic and electronic properties of RT_2 Laves phase compounds (R = Zr, Y, rare earth and T = transition metal) have been intensively studied [1–3]. Hydrogen absorption in these Laves phases induces an increase of the cell volume accompanied in some systems by structural distortions caused by hydrogen order. The magnetic properties of these compounds are very sensitive to changes of interatomic distances related to H insertion but also to the modification of

[4] Author to whom any correspondence should be addressed.

the electronic properties characterized by the formation of a low lying T–H band and the filling of the conduction band. Among these systems, the RFe_2 Laves phases compounds (R = Y and heavy rare earth) form several hydrides or deuterides with different structures for concentrations ranging between 1.3 and 5 H(D)/fu [4–9]. A large number of structural and magnetic studies performed for $x \leqslant 3.5$ H(D)/fu have shown a decrease of the Curie temperature and an increase of the Fe moment as the hydrogen content increases [4, 7, 10–15]. For $x \approx 4$ H(D)/fu, different results were found concerning the magnetic behaviour of the Fe sublattice depending on the R element: for R = Y an increase of the Fe moment was observed [16, 17] whereas for R = Er and Dy a sharp reduction of the Fe moment was found [17–19]. Recent works on $YFe_2D_{4.2}$ indicated that for this D content, the Fe moment is close to the ferromagnetic instability and that a transition from a ferromagnetic to an antiferromagnetic state occurs around 90 K [20]. Finally, applying high hydrogen or deuterium gaseous pressure allowed 5 H/(D)fu to be reached in YFe_2 and $ErFe_2$, where a strong reduction of the Fe moment in both compounds was found [9].

$ZrFe_2$ displays a different behaviour towards hydrogen absorption compared to the other RFe_2 compounds. For pressures up to 7 MPa, the amount of absorbed hydrogen is limited to 0.35 H/fu [21]. The application of high hydrogen or deuterium pressure ($P = 0.35$ GPa), however, allowed preparation of $ZrFe_2H(D)_{3.5}$ [22]. This compound crystallizes in the C15-type cubic structure and is ferromagnetic with a larger Fe moment at 4.2 K (2.2 μ_B/Fe) than the starting intermetallic $ZrFe_2$ (1.8 μ_B/Fe) [22, 23]. The study of $ZrFe_2H(D)_x$ formation and decomposition shows that no intermediate compound is formed between $x = 0.35$ and 3.5 [23]. On the other hand, applying pressures up to 1 GPa did not allow a larger H or D content to be obtained in $ZrFe_2$.

The aim of this study was to understand more clearly the competitive influence of the volume and T–D chemical bonding effect on the Fe magnetization in RFe_2D_x deuterides for large deuterium content ($3.5 \leqslant x \leqslant 5$). Since Y and Zr are nonmagnetic, this allows us to follow selectively the influence of deuterium on the Fe magnetization. For this purpose, adding to previous bulk magnetization and neutron diffraction measurements, we have performed ^{57}Fe Mössbauer spectroscopy experiments, which have already been used to characterize the local Fe magnetic order in a large number of metal hydrides or deuterides of the RFe_2, R_2Fe_{17} and $RFe_{11}T$ [18, 19, 24–36] type of compounds. Previous studies on YFe_2D_x compounds with $1.3 \leqslant x \leqslant 3.5$ by EXAFS and Mössbauer spectroscopy have shown the influence of the large Fe–Fe distance distribution induced by deuterium absorption on the local Fe magnetization [29, 31, 37, 38].

In this paper we will present at first results concerning the analysis of the structural data on $ZrFe_2D_{3.5}$, $YFe_2D_{3.5}$, $YFe_2D_{4.2}$ and YFe_2D_5 including new results based on synchrotron radiation and neutron diffraction experiments for $YFe_2D_{3.5}$. Then, the ^{57}Fe Mössbauer spectroscopy results obtained on these four compounds will be analysed in relation to these structural data. The relative influence of the cell volume increase, the Fe–Fe distribution and the Fe–H bonding on the local Fe magnetization will be discussed.

2. Experimental details

The YFe_2 and $ZrFe_2$ alloys were prepared by induction melting of the appropriate amount of metals under argon atmosphere followed by an adapted annealing treatment [6, 22]. The homogeneity and composition of the alloys were checked by means of x-ray diffraction (XRD) and microprobe analysis.

$YFe_2D_{3.5}$ and $YFe_2D_{4.2}$ were synthesized using a volumetric method with deuterium pressure below 1 MPa. To obtain $ZrFe_2D_{3.5}$ and YFe_2D_5, the RFe_2 samples were put in the high pressure apparatus described previously [22] and treated at 373 K in vacuum before the

hydrogen charging procedure was carried out. The hydrogenation was usually performed at pressures up to 1.0 GPa and temperatures up to 373 K for 2–5 days. In order to avoid possible hydrogen desorption the apparatus was cooled down to 213 K; then the pressure was reduced to atmospheric value and the samples were immediately transferred to liquid nitrogen.

The XRD measurements were performed at room temperature by using a D8 Brucker diffractometer (Cu Kα wavelength) in the range $10° < 2\theta < 120°$ with a step width of 0.02°. The XRD pattern of $YFe_2D_{3.5}$ at 290 K was measured using synchrotron radiation ($\lambda = 0.747\,44$ Å) provided by the Swiss–Norwegian Beamline at the ESRF (Grenoble). The neutron powder diffraction (NPD) pattern of $YFe_2D_{3.5}$ at 290 K was measured at the LLB (Saclay), using the 3T2 diffractometer with a wavelength of 1.225 Å. The patterns were refined with the FULLPROF code.

The ^{57}Fe Mössbauer spectra were recorded between 4.2 and 300 K using a conventional constant acceleration type of spectrometer. The data were analysed by superposing a set of discrete Lorentzians with equal width. The quadrupole interaction was treated as a perturbation to the magnetic hyperfine interaction. The isomer shift (δ) data are given relative to the source (Fe(Rh)) and are related to δ (relative to α-Fe at room temperature) by adding 0.12 mm s^{-1}. The errors on the hyperfine parameters are approximately ± 0.1 T for the hyperfine field and ± 0.01 mm s^{-1} for both the isomer shift and the quadrupole shift.

3. Results and discussion

3.1. Structural properties

3.1.1. $ZrFe_2D_{3.5}$. The structural study of $ZrFe_2D_{3.5}$ by means of XRD and NPD published in [23] indicated that the deuteride keeps the cubic C15 structure of the parent $ZrFe_2$ compound with an increase of 7.1% of the cell parameter and 22.6% of the cell volume. In the related patterns there was no indication of lattice distortion or superstructure lines [23]. The Wigner–Seitz (WS) cell volumes were calculated with the BLOKJE program from Gelato [39] using Voronoi polyhedra and considering only metallic atoms in order to estimate the pure volume effect (table 1). The results show that deuterium absorption induces a larger increase of the WS volume around the Fe atoms than around the Zr atoms. This difference is related to the difference of atomic radii between Zr and Fe atoms, since the volume of the polyhedra calculated without atomic radii around Zr and Fe lead to the same value of $\Delta V/V$ (22.6%). This can be explained by the fact that in $ZrFe_2$ the Fe–Fe distances ($d = 2.50$ Å) are close to the sum of the Fe atomic radii ($d = 2.52$ Å) whereas the Zr–Zr distances ($d = 3.06$ Å) are shorter than the sum of the Zr atomic radii ($d = 3.20$ Å). As the cell volume increases due to D absorption, the WS volume expansion is larger around Fe atoms than around Zr atoms. If all the A2B2 sites (pseudotetrahedral interstitial sites constituted of two R (A) and two Fe (B) atoms surrounding the D atom) were occupied by D atoms, the total D content would be 12 D/fu and each Fe would be surrounded by 12 D at 1.74 Å. Since there are only 3.5 D/fu instead of 12 D/fu, this means that there is an average of 3.5 D neighbours around each Fe site. Although no long range order of D atoms is observed (at least down to 10 K), locally a short range order of D site occupancy should occur due to repulsive interactions between D atoms. According to the Switendick criterion [40] and interatomic distance calculations, the occupancy of one A2B2 site in $ZrFe_2D_{3.5}$ excludes three other A2B2 interstitial sites located at distances shorter than 2 Å. In addition, assuming that the number of D neighbours should be an integer, each Fe should have at least either three or four D first neighbours.

3.1.2. $YFe_2D_{3.5}$. The $YFe_2D_{3.5}$ XRD pattern at 290 K was at first refined in the rhombohedral $R\bar{3}m$ space group with $a = 5.627(1)$ Å and $c = 13.352(4)$ Å [41]. Nevertheless, the analysis

Table 1. The cell volume (V/fu) and Wigner–Seitz cell volume (WS) for each R and Fe site in RFe_2D_x compounds calculated taking only metallic neighbours [39]. The structure and cell parameters were refined from the x-ray diffraction patterns (with synchrotron radiation for $x = 3.5$ and 4.2) registered at 290 K. The Goldschmidt atomic radii used for the calculation are $r_{Zr} = 1.60$ Å, $r_Y = 1.81$ Å and $r_{Fe} = 1.26$ Å.

Compound Structure	$ZrFe_2$ Cubic	$ZrFe_2D_{3.5}$ Cubic	YFe_2 Cubic	$YFe_2D_{3.5}$ Monoclinic	$YFe_2D_{4.2}$ Monoclinic	YFe_2D_5 Orthorhombic
Space group	$Fd\bar{3}m$	$Fd\bar{3}m$	$Fd\bar{3}m$	$C2/m$	$C2/m$	$Pmn2_1$
a (Å)	7.070	7.567	7.356	9.482	9.429	5.437
b (Å)				5.633	5.737	5.850
c (Å)				5.494	5.508	8.083
β (deg)				123.84	122.37	
V/fu (Å^3)	44.17	54.16	49.75	60.94	62.91	64.27
$\Delta V/V$ (%)		22.6		22.5	26.5	29.2
R atom WS volume (Å^3)	21.16	25.26	26.83	31.64	32.51	Y1:33.16 Y2:33.07
$\Delta V_R/V$ (%)		19.4		17.9	21.2	23.4
Fe atom WS volume (Å^3)	11.51	14.45	11.46	Fe1: 14.62 Fe2: 14.64 Fe3: 14.66	Fe1: 15.24 Fe2: 15.19 Fe3: 15.19	Fe1: 15.58 Fe2: 15.57 Fe3: 15.59
$\Delta V_{Fe}/V$ (%)		25.5		27.8	32.7	36.0

of the synchrotron radiation pattern of $YFe_2D_{3.5}$ at 290 K indicates a lowering of the crystal symmetry in the monoclinic $C2/m$ space group with $a_m = 9.4817(3)$ Å, $b_m = 5.6332(3)$ Å, $c_m = 5.4942(3)$ Å and $\beta = 123.84°$ with 1 Y (4e) and 3 Fe (2b, 2c and 4e) sites. To refine the $YFe_2D_{3.5}$ NPD pattern, however, it was necessary to consider a further lowering of the crystal symmetry in the $P2_1/c$ primitive monoclinic subgroup using the setting No 14_1 which corresponds to the unique axis b, cell choice 1 in the *International Tables for Crystallography* [42] and a doubling of the cell parameter a. This leads to the following monoclinic cell: $a = 15.754(2)$ Å, $b = 5.633(1)$ Å, $c = 9.476(1)$ Å and $\beta = 144.55°$. In this structure there are 2 Y, 5 Fe, 24 A2B2 and 8 AB3 (pseudotetrahedral interstitial sites constituted of one R (A) and three Fe (B) atoms surrounding the D atom) possible D sites. Since the lowering of the crystal symmetry in the $P2_1/c$ space group is only due to the interstitial deuterium atoms, the positions of the Y and Fe atoms which were derived from the refinement of the synchrotron radiation pattern have been fixed (see for example the crystal structure analysis of $ErFe_2D_5$ [43]). The structural parameters reported in table 2 show that only 15 A2B2 interstitial sites are partially occupied. The calculated WS cell volume indicates a larger cell volume increase around the Fe atoms compared to the Y atoms, but the differences between the different Fe sites remains small. The calculated interatomic distances and number of Fe and D nearest neighbours for each Fe atom are reported in table 3. The distances were calculated between all possible sites in the structure and then grouped for the same type of atom when the distances were the same. The corresponding coordination numbers were calculated taking into account the multiplicity of the site and the occupancy factors. Each Fe is surrounded by 6 Fe at distances between 2.75 and 2.81 Å and by 3–4 D atoms between 1.60 and 1.76 Å. The non-integer values of D neighbours are related to the fact that the occupancy numbers of the D sites are partial, which is common in the metal hydride, despite the observed very low crystal symmetry.

3.1.3. $YFe_2D_{4.2}$. Like that of $YFe_2D_{3.5}$, the synchrotron radiation pattern of $YFe_2D_{4.2}$ at 290 K was refined in a monoclinic structure ($C2/m$ space group) with $a_m = 9.4291$ Å, $b_m =$

Table 2. Crystallographic data for $YFe_2D_{3.5}$ refined from the NPD pattern at 290 K. The positions of the Y and Fe atoms were first refined in the $C2/m$ space group (SR pattern) and then fixed in the $P2_1/c$ space group.

Structure:	Monoclinic	Space group:	$P2_1/c$		
$a = 15.754(2)$ Å	$b = 5.633(1)$ Å	$c = 9.476(1)$ Å	$\beta = 144.55°$	$V = 487.6(1)1$ Å^3	
Atom (Wyckoff)	x	y	z	N	B (Å^2)
Y1(4e)	0.0625	0.000	0.250	1	1.219(6)
Y2(4e)	0.5625	0.000	0.250	1	
Fe1(4e)	0.250	0.000	0.000	1	
Fe2(2c)	0.000	0.000	0.500	1	
Fe3(2d)	0.500	0.000	0.500	1	1.033(4)
Fe4(4e)	0.250	0.250	0.750	1	
Fe5(4e)	0.750	0.250	0.750	1	
D1(4e)	0.225(12)	0.000	0.302(18)	0.16(1)	
D2(4e)	0.055(3)	0.215(4)	0.450(4)	0.75(1)	
D3(4e)	0.428(2)	0.164(4)	0.515(4)	0.77(1)	
D4(4e)	0.953(2)	0.190(4)	0.561(3)	0.90(1)	
D5(4e)	0.164(3)	−0.003(6)	0.192(4)	0.61(1)	
D6(4e)	0.694(5)	0.009(10)	0.235(8)	0.33(1)	0.356(4)
D7(4e)	0.533(3)	0.271(5)	0.491(5)	0.55(1)	
D8(4e)	0.381(5)	0.139(8)	0.100(7)	0.35(1)	
D9(4e)	0.826(4)	0.133(5)	0.011(6)	0.50(1)	
D10(4e)	0.658(3)	0.180(5)	0.979(6)	0.60(1)	
D11(4e)	0.303(6)	0.723(9)	0.993(10)	0.31(1)	
D12(4e)	0.746(3)	0.723(5)	0.873(4)	0.44(1)	
D13(4e)	0.774(4)	0.723(5)	0.127(4)	0.28(1)	
D14(4e)	0.546(3)	0.593(6)	0.241(5)	0.54(1)	
D15(4e)	0.938(4)	0.617(8)	0.255(8)	0.38(1)	
D/fu				3.7(2)	
$R_{wp} = 9.27\%$	$R_I = 9.34\%$	$\chi^2 = 1.28$			

Table 3. The number of Fe–Fe and Fe–D nearest neighbours and interatomic distances in $YFe_2D_{3.5}$. The standard deviation is calculated to be 0.001 Å on the Fe–Fe distances and 0.02 Å on the Fe–D distances.

Fe site	N_{Fe}	d_{Fe-Fe} (Å)	Total N_{Fe}	$\langle d_{Fe-Fe}\rangle$ (Å)	Total N_D	$\langle d_{Fe-D}\rangle$ (Å)
Fe1(4e)	4	2.756	6	2.753	3.3(1)	1.72
	2	2.748				
Fe2(2c)	4	2.811	6	2.790	4.0(1)	1.71
	2	2.748				
Fe3(2d)	4	2.811	6	2.790	3.7(1)	1.67
	2	2.748				
Fe4(4e)	4	2.813	6	2.794	3.3(1)	1.66
	2	2.756				
Fe5(4e)	4	2.813	6	2.794	4.0(1)	1.76
	2	2.756				
⟨Fe⟩			6	2.784	3.6(2)	1.71

5.7374 Å, $c_m = 5.5078$ Å and $\beta_m = 122.372°$ [20]. The NPD pattern at the same temperature has been refined in a primitive monoclinic cell ($P2_1/c$ space group, unique axis c, cell choice 1) [44]. In this structure there are: 1 Y site, 3 Fe sites (Fe1 (2b), Fe2 (2c) and Fe3 (4e)),

3.5(1) D atoms located in 9 out of 12 possible A2B2 sites and 0.5(1) D atoms in 2 out of 4 AB3 sites. The analysis of each Fe site environment indicates 6 Fe neighbours at distances between 2.75 and 2.87 Å and only small differences of the WS cell volume. However, each Fe site has a significantly different number of D neighbours: on average there are 3.2 D around Fe1, 4.4 D around Fe2 and 5.2 D around the Fe3 site.

A very close examination of the NPD pattern indicated weak additional lines which can be indexed by doubling the monoclinic cell along the b axis. To refine this superstructure, there are several possibilities—for example in a $P2/m$ space group with 4 Y, 8 Fe, 48 A2B2 and 16 AB3 sites—but due to the weakness of the superstructure lines and the large number of D sites (192 positions and 64 occupancy numbers), it was not possible to refine the NPD pattern is this superstructure. Nevertheless, it is expected that this lowering of crystal symmetry will influence the number of Fe sites observed by Mössbauer spectroscopy.

The structural evolution of $YFe_2D_{4.2}$ below room temperature shows a 0.5% cell volume increase around 83 K, attributed to a magnetoelastic transition. The neutron diffraction analysis shows a ferromagnetic structure from 1.5 to 80 K, an antiferromagnetic structure from 80 to 132 K and a paramagnetic state above 132 K.

3.1.4. YFe_2D_5. YFe_2D_5 crystallizes at 290 K in an orthorhombic $Pmn2_1$ space group with $a_0 = 5.427(1)$ Å, $b_0 = 5.828(1)$ Å and $c_0 = 8.056(1)$ Å [9]. In this structure there are 2 Y sites (2a, 2a) and 3 Fe sites (2a, 2a, 4b). The Fe–Fe distance distribution indicates that each Fe is surrounded by 6 Fe neighbours at distances between 2.66 and 2.95 Å. The WS cell volumes are very similar for each of the Fe sites (table 1). Previously, the NPD pattern of $ErFe_2D_5$ was refined in the $Pmn2_1$ space group with 3.75 D in 6 out of 14 A2B2 sites and 0.87 D in 2 out of 6 AB3 sites [43]. Since YFe_2D_5 is isostructural to $ErFe_2D_5$, it can be assumed that the D atoms in YFe_2D_5 occupy the same interstitial sites with occupancy numbers similar to those for $ErFe_2D_5$. These data are then used to calculate the average number of D neighbours around each Fe site in YFe_2D_5. Considering either refined or (integer) D site occupancies we obtained 5.4 (5) D around Fe1, 4.6 (5) D around Fe2 and 4.9 (5) D around Fe3 with Fe–D distances between 1.65 and 1.80 Å.

3.2. Mössbauer studies

3.2.1. $ZrFe_2D_{3.5}$. Despite the fact that neutron diffraction data show C15 structure for both $ZrFe_2$ and $ZrFe_2D_{3.5}$, the difference between the Mössbauer spectra of the deuteride and of the parent compound is obvious (figure 1). In the cubic C15 structure a single crystallographic site (8a) with trigonal symmetry around one of the [111] directions (identical to the principal axes of the electric field gradient (EFG)) is available for the Fe atoms (corner sharing tetrahedra network). Since in the Hamiltonian, for a combined electrostatic and magnetic hyperfine interaction a term $3\cos^2\theta - 1$ is present (θ being the angle between the principal axis of the EFG tensor and the hyperfine field), the crystallographically identical sites may become magnetically inequivalent if the easy axis of magnetization is not oriented along the [001] direction. In the case of a [111] easy axis, a ratio of 3:1 is obtained for the inequivalent sites, corresponding to the angles $\theta = 70.5°(3\times)$ and $0°(1\times)$ [4, 5]. In fact, two sextets with an area ratio 3:1 are observed for $ZrFe_2$ (figure 1, top, and table 4).

The drastic change of the Mössbauer spectrum observed for the deuteride (figure 1, bottom) is attributed to a change of the easy axis of magnetization away from a principal crystallographic axis as well as to the incomplete deuterium occupation at the 96 g A2B2 sites, generating changes of the local environment of the Mössbauer atoms. In a first attempt, four sextets with equal intensity, arising from the four iron atoms forming a tetrahedron in the C15 structure (which are now magnetically inequivalent), were assumed, yielding a reasonable fit to the

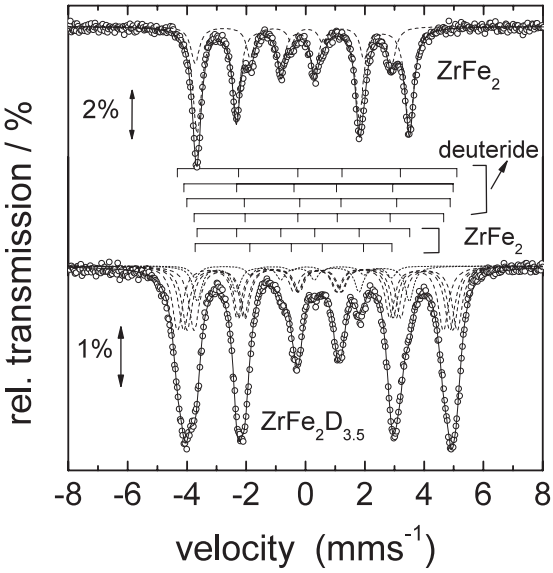

Figure 1. Mössbauer spectra of $ZrFe_2$ and $ZrFe_2D_{3.5}$ at 4.2 K; ○—experimental points; dashed curves—individual subspectra; solid line—total spectrum; the stick diagram on top of the $YFe_2D_{3.5}$ spectrum indicates the line positions.

Table 4. Hyperfine parameters derived from the computer fit described in the text for $ZrFe_2$ and $ZrFe_2D_{3.5}$ at various temperatures.

$ZrFe_2$							
T (K)	Site/θ (deg)	δ (mm s^{-1})	$\langle\delta\rangle$	Δ (mm s^{-1})	$\langle\Delta\rangle$	B_{hf} (T)	$\langle B_{hf}\rangle$
4.2	70.5	−0.17	−0.17	0.18	0.02	22.23	21.82
	0	−0.18		−0.47		20.57	
100	70.5	−0.20	−0.20	0.19	0.04	21.50	21.15
	0	−0.21		−0.40		20.10	
295	70.5	−0.30	−0.30	0.17	0.05	20.07	19.77
	0	−0.29		−0.30		18.85	
$ZrFe_2D_{3.5}$							
T (K)	Sextet	δ (mm s^{-1})	$\langle\delta\rangle$	Δ (mm s^{-1})	$\langle\Delta\rangle$	B_{hf} (T)	$\langle B_{hf}\rangle$
4.2	1	0.44	0.43	−0.08	0.00	29.30	27.79
	2	0.38		0.11		28.20	
	3	0.47		−0.05		27.53	
	4	0.43		0.03		26.11	
100	1	0.39	0.41	0.00	0.00	28.95	27.45
	2	0.40		−0.04		27.62	
	3	0.44		0.05		27.42	
	4	0.39		0.02		25.81	
295	1	0.30	0.25	−0.03	0.00	25.37	23.72
	2	0.24		0.03		24.88	
	3	0.26		0.01		22.95	
	4	0.20		−0.02		22.99	

experimental data. If, however, the number of sextets is increased to five, the quality of the fit is somewhat improved, with only minor changes if the number of sextets is increased further. Thus, one may conclude that, at least on a microscopic scale, the varying local deuterium environment leads to an, albeit narrow, hyperfine field distribution. In order to account for the

Table 5. Hyperfine parameters obtained for $YFe_2D_{3.5}$ and $YFe_2D_{4.2}$ at 4.2 K.

Compound	Fe site[a]	N_{occ}	δ (mm s^{-1})	Δ (mm s^{-1})	B_{hf} (T)	$\langle\delta\rangle$ (mm s^{-1})	$\langle\Delta\rangle$ (mm s^{-1})	$\langle B_{hf}\rangle$ (T)
$YFe_2D_{3.5}$	Fe3	2	0.35	0.28	30.27			
	Fe1	4	0.28	0.03	29.23			
	Fe4	4	0.34	−0.10	27.86	0.34	0.07	26.68
	Fe2	2	0.54	0.17	23.81			
	Fe5	4	0.29	0.11	23.58			
$YFe_2D_{4.2}$		1	0.39	−0.05	27.96			
		1	0.47	0.30	27.22			
		1	0.50	0.01	26.53			
		1	0.52	0.22	19.33	0.49	0.07	20.68
		1	0.52	−0.04	18.33			
		1	0.37	−0.47	16.18			
		1	0.58	0.43	15.11			
		1	0.53	0.12	14.76			

[a] For the attribution of the Fe sites, see the text.

presence of some parent $ZrFe_2$, a weak (13 at.% at 4.2 K and at 100 K) pattern (consisting of two sextets with the area ratio 3:1) had to be added (figure 1, bottom). At ambient temperature its absorption area has remarkably increased at the expense of the deuteride phase up to 30% (figure 2), probably due to deuterium desorption upon heating. The linewidth of the sextets obtained at 4.2 K for the deuteride is 0.41 mm s^{-1}, compared to 0.35 mm s^{-1} observed for the parent phase, which supports the above assumption about the local environment fluctuation of a Mössbauer atom.

Since the cubic C15 structure is preserved upon hydrogen uptake, the different hyperfine fields B_{hf} (table 4) are supposed to reflect the specific deuterium environment. From the small values of the quadrupole interaction a direction of the magnetization close to [001] might be suggested under the assumption that in the deuteride the orientation of the principal axis of the EFG [111] has not been altered. The change in isomer shift upon temperature change is solely due to the second-order Doppler effect.

The deuterium induced increase in isomer shift of +0.60 mm s^{-1} (table 4) is unusually large, particularly since the rise in volume (22.6%) is within the range generally observed upon charging in this type of intermetallic compound (3 Å/D atoms). If the total change in isomer shift obtained by Mössbauer spectroscopy is separated according to Wagner and Wortmann [45] into a volume contribution (estimated from high pressure data obtained from α-Fe) and an electronic contribution, the latter can be estimated. The value of 0.60 mm s^{-1} corresponds to a reduction of the (s electron) charge density at the Fe nucleus of about 0.3–0.4 s electrons (Walker *et al*) [46], thus exceeding the values usually obtained in the case of R–Fe hydrides/deuterides [4, 5]. Therefore, in the case of $ZrFe_2D_{3.5}$, both the volume and electronic contribution to the isomer shift have to be considered, pointing to some importance of a charge transfer to/from Fe. The rise in B_{hf} of almost 6 T (27%) upon deuterium uptake is in reasonable agreement with the increase of the Fe moment observed by means of neutron diffraction (0.4 μ_B, i.e. 22%) [23].

3.2.2. YFe_2D_x. YFe_2 deuterides with various D concentrations ($x = 3.5$, 4.2 and 5) were studied. The spectrum obtained from $YFe_2D_{3.5}$ significantly differs from the Zr equivalent (figure 3). Following the results from neutron diffraction, the spectra were fitted with five components (table 5) resulting from the inequivalent Fe sites Fe1–Fe5 with an intensity ratio of 2:2:4:4:4. At 4.2 K the individual hyperfine fields differ by about 6 T (20%). This variation

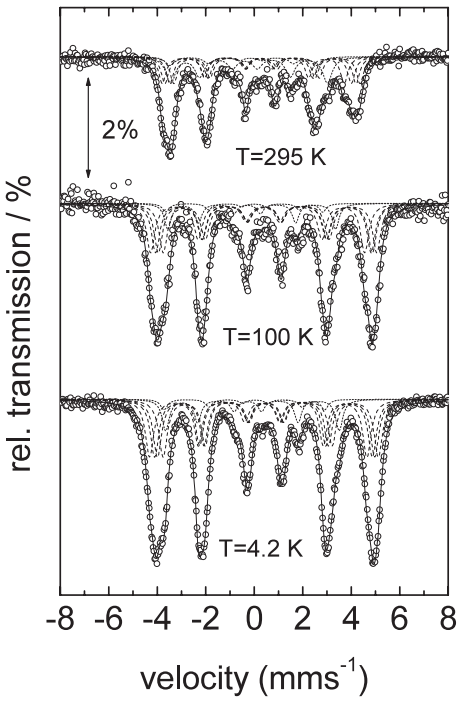

Figure 2. Mössbauer spectra recorded from $ZrFe_2D_{3.5}$ at various temperatures; ○—experimental points; dashed curves—individual subspectra; solid curve—total spectrum.

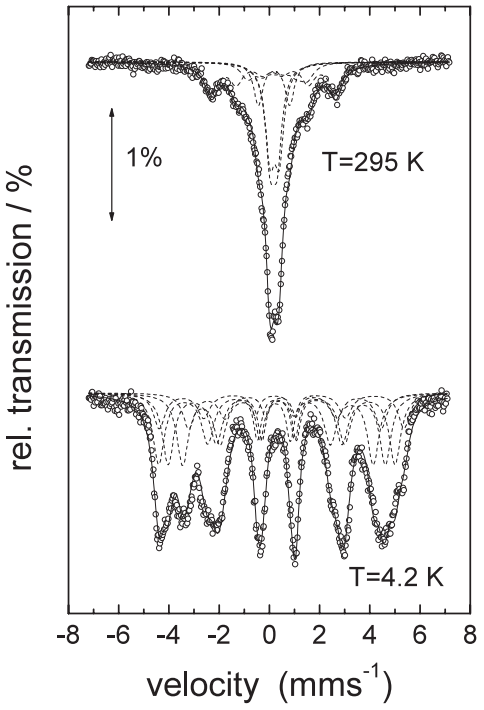

Figure 3. Mössbauer spectra recorded from $YFe_2D_{3.5}$ at 4.2 and 295 K; ○—experimental points; solid curve—total spectrum; dashed curves—subspectra.

cannot be simply explained by the changes of the Fe–Fe distances and the calculated WS volume (table 1), since, while the Fe1 site has slightly shorter distances, the four other sites have almost the same Fe environment. Therefore the difference of D neighbours has to be considered. The average number of D atoms varies between 3.3 and 4 and the distances between 1.66 and 1.76 Å. From magnetic measurements, we know that the saturation magnetization at 4.2 K of YFe_2D_x compounds reaches a maximum for $x = 3.5$ and decreases for $x > 3.5$. If we assume that the number of D neighbours around each Fe atom has the same influence on the Fe moment, taking into account the multiplicity of each Fe site in $YFe_2D_{3.5}$ it is possible to attribute each Fe site to one sextet (table 5). Following this assumption the Fe3 site (3.7 D) should have the largest hyperfine field (30.27 T) whereas the Fe2 and Fe5 sites (4.0 D) should have the lowest (23.81 and 23.58 T). The distribution of the isomer shift values (0.28 mm $s^{-1} < \delta <$ 0.54 mm s^{-1}) cannot be simply explained by the geometric effect of the local environment, and should also be related to the D distribution around each Fe site, but in a different way to the hyperfine field. The mean hyperfine field of 26.68 T is substantially larger than for the starting intermetallic: 21.36 T. This 25% increase is smaller than the 48% magnetization enlargement from 2.9 to 4.3 μ_B/fu observed as x increases from 0 to 3.5. However, band structure calculations [47–49] and NMR spin echo ^{89}Y measurements [50] have shown that in YFe_2, Y has a moment of $-0.45\ \mu_B$ induced by the polarization of the s conduction electrons by means of the Fe moment which reduces the total magnetization. Therefore the Fe moment in YFe_2 is about 1.67 μ_B/Fe or 3.35 μ_B/fu. If in $YFe_2D_{3.5}$ the saturation magnetization results only from the Fe moments, an increase of 28% close to that observed by Mössbauer spectroscopy is obtained.

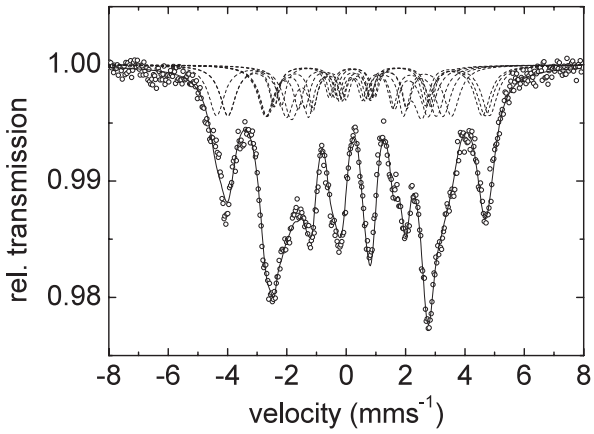

Figure 4. Mössbauer spectra recorded from $YFe_2D_{4.2}$ at 4.2 K; ○—experimental points; dashed curves—individual subspectra; solid curve: total spectrum. The spectrum has been fitted by superposing eight sextets with equal intensity (see table 5).

At room temperature, the hyperfine fields arising from three Fe sites among five have already collapsed (figure 3, top). This is due to the fact that for $YFe_2D_{3.5}$ at this temperature the Curie point (340 K) is approached. As has already been observed in several cases [51, 52] the hyperfine fields as a function of temperature vanish over a broad interval, demonstrating the crucial influence of the local environment on the hyperfine interactions.

The spectrum recorded from $YFe_2D_{4.2}$ at 4.2 K has been refined with eight sextets of the same intensity (figure 4), in agreement with the proposed superstructure (section 3.1.3). The broad distribution of isomer shifts (0.37 mm $s^{-1} < \delta < 0.58$ mm s^{-1}) and of hyperfine fields (15 T $< B_{hf} <$ 28 T) points to a strongly varying local environment of the Fe atoms (table 5). The calculated Fe–Fe distance distribution and WS volume cannot explain this broad distribution. Therefore here also the D surrounding has to be considered. Although, it is not possible to assign each sextet to an Fe site, since the superstructure could not be resolved from NPD data, one can consider in comparison with $YFe_2D_{3.5}$ that five among eight Fe sites are surrounded by more than four D per fu. The crystallographic data obtained from the refinement in the primitive monoclinic cell ($P2_1/c$) indicate that the Fe3 site (4e) has about five D neighbours. Therefore most of the Fe sites which have the lower hyperfine field should be derived from the Fe_3 site after the lowering of crystal symmetry.

The mean B_{hf} of 20.68 T, lying close to that of YFe_2, is lower than that obtained for $YFe_2D_{3.5}$. This reduction of $B_{hf,}$, in agreement with the decrease of the saturation magnetization ($M_s = 3.7\ \mu_B$/fu) observed above a critical deuterium concentration, is attributed to a decrease of the DOS at the Fermi level due to the shift of the Fe 3d band toward the valence band [53]. This means that the chemical Fe–D bonding becomes predominant towards the pure volume effect which leads to an increase of the Fe moment [53, 54].

In order to follow the evolution of the magnetic hyperfine interaction in $YFe_2D_{4.2}$, the Mössbauer spectra were measured at several temperatures ranging from 4.2 K up to 300 K with narrow temperature intervals near the magnetovolumic transition around 90 K (figure 5). Between 4.2 and 90 K (figure 5, lower) the overall shape of the spectra remains similar with a progressive and smooth decrease of the hyperfine field as the temperature increases. In this temperature range all the spectra could be reasonably refined with eight sextets with equal intensities. This agrees with the ferromagnetic behaviour observed from magnetization measurements and neutron diffraction experiments between 4.2 and 90 K. At 90 K, magnetic

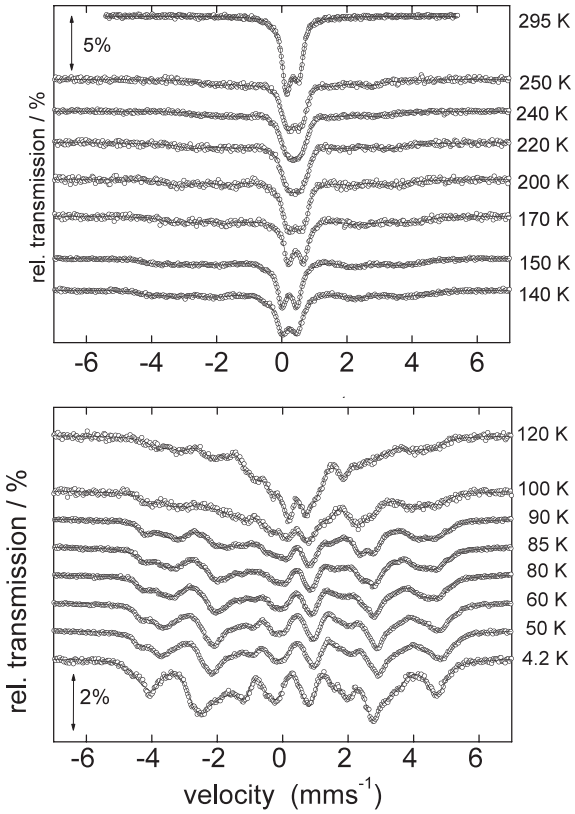

Figure 5. Mössbauer spectra recorded from $YFe_2D_{4.2}$ at various temperatures between 4.2 and 300 K; ○—experimental points; solid curve—total spectrum.

measurements have shown a sharp decrease of the magnetization associated with a 0.55% volume reduction.

Between 100 and 120 K, a more complex pattern is observed showing a partial collapse of the Fe hyperfine field (figure 5, lower). This temperature interval corresponds to the range of existence of an antiferromagnetic structure observed in the NPD pattern of $YFe_2D_{4.2}$ [20]. In addition, the strong magnetic field dependence of the $M(H)$ magnetization curves observed above 90 K is similar to the itinerant electron metamagnetic (IEM) behaviour found in RCo_2 compounds [55–57].

In order to interpret the results obtained from magnetic measurements, neutron diffraction and Mössbauer spectroscopy, it should be assumed that some of the Fe sites, which are surrounded by a large number of D atoms, are very close to the ferromagnetic instability. At 4.2 K their hyperfine field (15 T $< B_{hf} <$ 20 T) is already smaller than in YFe_2. Near 90 K their Fe moments collapse, through an IEM behaviour. As a consequence the exchange interaction between the remaining three Fe moments is strongly modified and a ferromagnetic order cannot be maintained. The antiferromagnetic structure with a (0, 0.5, 0) propagation vector becomes more stable. As the temperature increases, the magnitudes of the Fe1 and Fe2 moments decrease progressively up to 130 K. Above 140 K, the Mössbauer spectra are dominated by a broadened doublet, most probably due to a distribution of electric field gradients. The remaining weak sextet could be due to some amount of $YFe_2D_{3.5}$ as observed in the XRD patterns. According to the structural considerations at 295 K the Mössbauer spectra

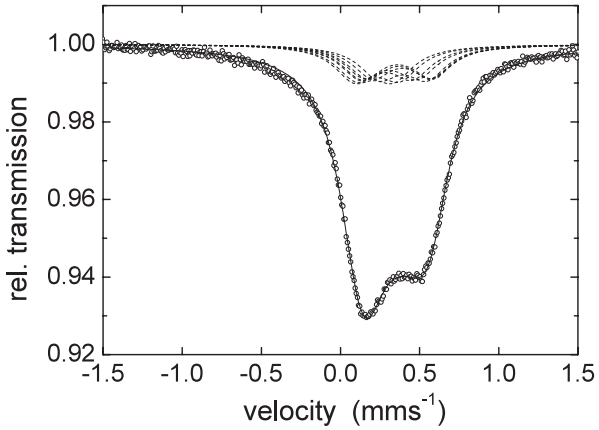

Figure 6. Mössbauer spectra recorded from $YFe_2D_{4.2}$ at 295 K; ∘—experimental points; dashed curves—individual subspectra; solid curve: total spectrum. The spectrum has been fitted by superposing eight doublets with equal intensity.

Table 6. Individual isomer shifts (δ) and quadrupole shifts (Δ) and average values obtained for YFe_2D_5 between 4.2 and 200 K.

T (K)	N_{occ}	δ	$\langle\delta\rangle$ (mm s^{-1})	Δ	$\langle\Delta\rangle$
4.2	4	0.48		0.63	
	2	0.44	0.48	0.28	0.45
	2	0.50		0.27	
100	4	0.46		0.60	
	2	0.49	0.46	0.28	0.44
	2	0.43		0.27	
200	4	0.40		0.53	
	2	0.44	0.41	0.27	0.41
	2	0.38		0.30	

was refined with a distribution of eight doublets of equal intensity (figure 6). In order to reduce the number of free parameters, the quadrupole shift was constrained to increase linearly. The best fit was obtained with an increase of +0.05 mm s^{-1} per site. The isomer shift as a fitting parameter roughly followed the rise of the quadrupole shift, indicating a lower s electron density at the nuclear site with increasing EFG.

In YFe_2D_5 each Fe is in average surrounded by five D atoms. *Ab initio* band structure calculations have shown that for YFe_2D_5, due to the strong decrease of the DOS at the Fermi level, the Stoner criterion for the onset of ferromagnetism is no longer fulfilled [53]. This prevents the formation of magnetic order and, thus, of a magnetic hyperfine interaction, even at 4.2 K.

Mössbauer spectra were recorded at 4.2, 100 and 200 K. Following the structural studies the spectra were fitted by superposing three doublets with an intensity ratio of 1:1:2 corresponding to the Fe sites 2a, 2a, 4b (figure 7). The hyperfine parameters derived from fitting the spectra are given in table 6. The values of the individual isomer shifts and quadrupole shifts reflect the slightly different deuterium environments of the Fe sites. Again, the reduction of the isomer shift with raising temperature is due to the second-order Doppler shift. The weak temperature dependence of the quadrupole shift may be attributed to small changes in the lattice dimensions leading to an alteration of the electric field gradient at the Fe sites.

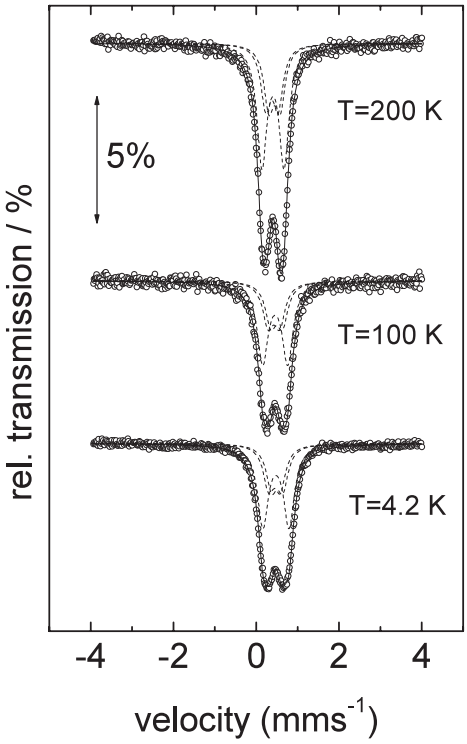

Figure 7. Mössbauer spectra recorded from YFe_2D_5 at various temperatures; ○—experimental points; dashed curves—individual subspectra; solid curve—total spectrum.

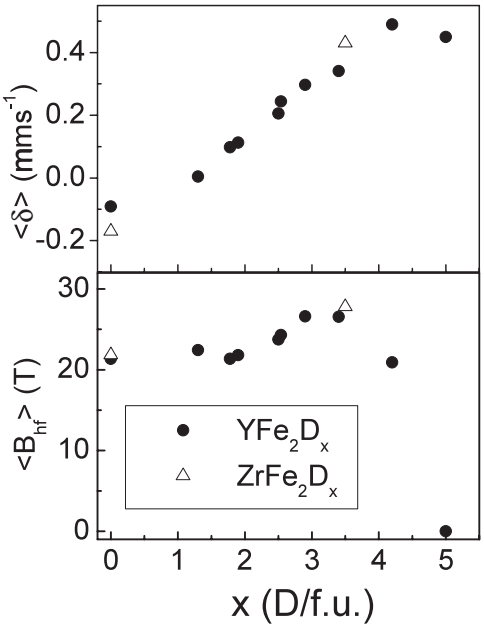

Figure 8. Mean ^{57}Fe isomer shift $\langle\delta\rangle$ and hyperfine field $\langle B_{\rm hf}\rangle$ versus D content obtained at 4.2 K for YFe_2D_x and $ZrFe_2D_x$.

3.3. Discussion

At first we will compare the behaviour of $ZrFe_2D_{3.5}$ and $YFe_2D_{3.5}$, then the influence of the D content in YFe_2D_x deuterides.

In $ZrFe_2D_{3.5}$ the increase of the mean ^{57}Fe isomer shift is related to both volume and electronic effects (charge transfer from/to Fe). In the YFe_2D_x deuterides no significant D–Fe charge transfer can be observed, leaving the deuterium induced change in isomer shift predominantly to the influence of the volume expansion (figure 8, top). For $ZrFe_2D_{3.5}$ the mean ^{57}Fe hyperfine field at 4.2 K is close to that observed for $YFe_2D_{3.5}$ (figure 8, bottom). However, at 4.2 K $YFe_2D_{3.5}$ shows a broader hyperfine field distribution than $ZrFe_2D_{3.5}$. This difference can be explained by a larger sensitivity of the Fe moment to the deuterium environment in the monoclinic $YFe_2D_{3.5}$ than in the cubic $ZrFe_2D_{3.5}$. The analysis of the crystal structure has shown that the average number of D neighbours varies between 3 and 4 in $YFe_2D_{3.5}$, whereas only an average value of 3.5 D can be found in $ZrFe_2D_{3.5}$. In $YFe_2D_{3.5}$, we are just below a critical D concentration above which the Fe moment decreases. For $ZrFe_2D_{3.5}$, since it was not possible to prepare a deuteride with $x > 3.5$, there is no way to know what the behaviour of the Fe moment will be for large D content in $ZrFe_2D_x$. However, since at ambient temperature $ZrFe_2D_{3.5}$ is still ferromagnetic, demonstrated by the presence of only sextets in the Mössbauer pattern whereas in $YFe_2D_{3.5}$ several hyperfine fields have already collapsed, this indicates that the Curie temperature of $ZrFe_2D_{3.5}$ is higher than that of $YFe_2D_{3.5}$. This is

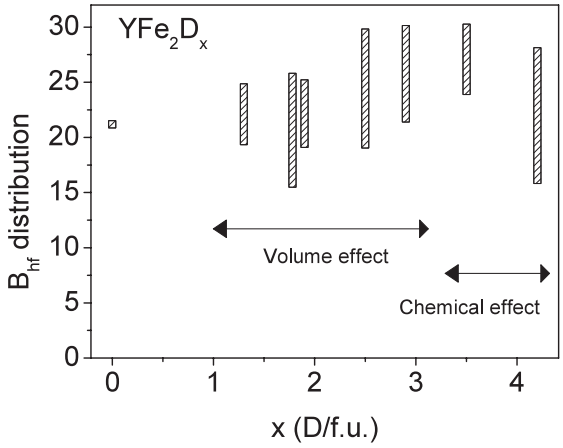

Figure 9. The B_{hf} distribution in YFe_2D_x compound measured at 4.2 K as a function of D content. The bars are plotted between the minimum and maximum B_{hf} values refined from ^{57}Fe Mössbauer spectra for each compound. The two domains called volume effect and chemical effect indicate the ranges where each effect is responsible for the B_{hf} distribution.

a strong indication that the Fe–Fe exchange interaction remains stronger in $ZrFe_2D_{3.5}$ than in $YFe_2D_{3.5}$. Although band structure calculations have yet not been performed for $ZrFe_2D_{3.5}$ one can expect that for this concentration the volumetric effect will still be the main effect leading to the large increase of the Fe moment.

In YFe_2D_x deuterides the mean ^{57}Fe isomer shift increases continuously with the D content in agreement with the cell volume expansion induced by deuterium atoms (figure 8, top). In agreement with the magnetization measurements, the evolution of the mean hyperfine field at 4.2 K (figure 8, bottom) indicates an increase up to $x = 3.5$, a decrease for $x = 4.2$ and a collapse for $x = 5$. This evolution has been explained by band structure calculations showing a competition between the volume effect which tends to localize the Fe moment and the Fe–H bonding leading to a lowering of the Fe moment [53]. A similar evolution of the mean B_{hf} has been observed for other RFe_2 hydrides. For example for $ErFe_2H_x$ and $DyFe_2H_x$ a strong decrease of B_{hf} was found between $x = 3.5$ and 4.1 [18].

The distribution of the hyperfine fields was often attributed to the variation of the number of H or D neighbours around the Fe atoms [13, 18, 19, 58]; nevertheless, the analysis of the Mössbauer data in relation with the structural and electronic properties of YFe_2D_x compounds seems to indicate that this influence should differ depending on the D content inside the Laves phases.

For a low D content ($1.3 \leqslant x < 3$) both XRD and EXAFS analysis have shown a broad Fe–Fe distance distribution [37], related to the fact that there is a strong relaxation of the Fe atom positions around the interstitial sites: the Fe–Fe distances contract towards an empty interstitial site and expand around a filled site. For example in $YFe_2D_{1.3}$ the Fe–Fe distances range from 2.45 to 3.2 Å ($d_{\mathrm{Fe-Fe}} = 2.60$ Å in YFe_2). In this case the B_{hf} distribution can be related to the volume effect: a larger hyperfine field corresponds to larger Fe–Fe distances around one Fe site. For $x = 3.5$ and 4.2 the B_{hf} distribution cannot be related to a broad distribution of the Fe–Fe distances, since these distances remain relatively similar for all the Fe sites, but rather to the large influence of the D environment which has a drastic influence on the Fe moment for such large concentration. The evolution of the hyperfine field distribution is illustrated in figure 9.

4. Conclusion

This study of the evolution of the local magnetic order in $ZrFe_2$ and YFe_2 with high deuterium content ($x \geqslant 3.5$) has shown that at 4.2 K the Fe moment first increases compared to that of the parent compound. Then, for a larger D content a sharp decrease of the Fe moment and of the magnetic ordering temperature is observed. This evolution can be related to a competition between volumetric effects which tend to localize the Fe moment and electronic effects leading to a filling of the conduction band and therefore to a strong decrease of the DOS for larger D content. This behaviour also influences strongly the hyperfine field distribution, which become sensitive to the number of D neighbours when reaching a large D content ($x > 3$).

Acknowledgments

We wish to express our thanks to Dr Patterson for his help with collecting the synchrotron radiation pattern on the Swiss–Norwegian Beamline at the European Synchrotron Radiation Facility (Grenoble, France) and to Mrs F Bourée for the neutron diffraction measurement at the Laboratoire Léon Brillouin (Saclay, France). We thank I Jacob for the preparation of the $ZrFe_2$ intermetallic compound.

References

[1] Buschow K H J 1976 *Solid State Commun.* **19** 421
[2] Yvon K and Fischer P 1988 Crystal and magnetic structures of ternary metal hydrides: a comprehensive review *Hydrogen in Intermetallic Compounds I* vol 63, ed L Schlapbach (Berlin: Springer) p 87
[3] Fukai Y 1993 Metal–hydrogen system under extended p, T conditions *The Metal–Hydrogen System, Basic Bulk Properties* vol 21, ed Y Fukai (Berlin: Springer) p 71
[4] Berthier Y, de Saxce T, Fruchart D and Vulliet P 1985 *Physica* B **130B** 520
[5] Wiesinger G and Hilscher G 1988 *Hydrogen in Intermetallic Compounds I* (*Springer Topics in Applied Physics* vol 63) ed L Schlapbach (Berlin: Springer) p 285
[6] Paul-Boncour V, Guénée L, Latroche M, Percheron-Guégan A, Ouladdiaf B and Bourée-Vigneron F 1999 *J. Solid State Chem.* **142** 120
[7] Paul-Boncour V and Percheron-Guégan A 1999 *J. Alloys Compounds* **293–295** 237
[8] Shashikala K, Raj P and Sathyamoorthy A 1996 *Mater. Res. Bull.* **31** 957
[9] Paul-Boncour V, Filipek S M, Percheron-Guégan A, Marchuk I and Pielaszek J 2001 *J. Alloys Compounds* **317/318** 83
[10] Fish G E, Rhyne J J, Sankar S G and Wallace W E 1979 *J. Appl. Phys.* **50** 2003
[11] Rhyne J J, Fish G E, Sankar S G and Wallace W E 1979 *J. Physique Coll.* **5** 209
[12] de Saxce T, Berthier Y and Fruchart D 1985 *J. Less-Common Met.* **107** 35
[13] Fruchart D, Berthier Y, de Saxce T and Vuillet P 1987 *J. Less-Common Met.* **130** 89
[14] Kanematsu K, Ohkubo N, Itoh K, Ban S, Miyajima T and Yamaguchi Y 1996 *J. Phys. Soc. Japan* **65** 1072
[15] Paul-Boncour V, Escorne M, Mauger A, Latroche M and Percheron-Guégan A 1996 *J. Appl. Phys.* **79** 4253
[16] Buschow K H J and van Diepen A M 1976 *Solid State Commun.* **19** 79
[17] Oesterreicher H and Bittner H 1980 *J. Magn. Magn. Mater.* **15–18** 1264
[18] Dunlap B D, Shenoy G K, Friedt J M, Viccario P J, Niarchos D, Kierstead H A, Aldred A T and Westlake D G 1979 *J. Appl. Phys.* **50** 7682
[19] Shashikala K, Raj P, Sathyamoorthy A, Chandrasekhar Rao T V, Siruguri V and Paranjpe S K 1999 *Phil. Mag.* B **79** 1195
[20] Paul-Boncour V, André G, Bourée F, Guillot M, Wiesinger G and Percheron-Guegan A 2004 *Physica* B **350** e27
[21] Shaltiel D, Jacob I and Davidov D 1977 *J. Less-Common Met.* **53** 117
[22] Filipek S M, Jacob I, Paul-Boncour V, Percheron-Guégan A, Marchuk I, Mogilyanski D and Pielaszek J 2001 *Pol. J. Chem.* **75** 1921
[23] Paul-Boncour V, Bourée F, Filipek S M, Marchuk I, Jacob I and Percheron-Guégan A 2003 *J. Alloys Compounds* **356/357** 69

[24] Viccaro P J, Shenoy G K, Dunlap B D, Westlake D G and Miller J F 1979 *J. Physique Coll.* **2** 198
[25] Viccaro P J, Friedt J M, Niarchos D, Shenoy G K, Aldred A T and Westlake D G 1979 *J. Appl. Phys.* **50** 2051
[26] Cohen R L, West K W, Oliver F and Buschow K H J 1980 *Phys. Rev.* B **21** 941
[27] Hrubec J, Steiner W and Reissner M 1983 *J. Magn. Magn. Mater.* **37** 93
[28] Deryagin A V, Moskalev A V, Mushinkov V N and Terentiev S V 1984 *Fiz. Met. Metalloved.* **57** 1086
[29] Deryagin A V, Kudrevatykh N V, Moskalev V N and Mushinkov V N 1984 *Phys. Met. Metalloved.* **58** 96
[30] Pszczola J, Zukrowski J, Krop K, Suwalski J, Kucharski Z and Lukasiak M 1985 *Physica* B **130B** 446
[31] Aït-Bahammou A, Hartmann-Boutron F, Meyer C, Gros Y and Berthier Y 1986 *Hyperfine Interact.* **28** 577
[32] Przewoznik J, Zukrowski J and Krop K 1998 *J. Magn. Magn. Mater.* **187** 337
[33] Coaquira J A H, Rechenberg H R and Mestnik Filho J 1999 *J. Alloys Compounds* **288** 42
[34] Bara J J, Bogacz B F, Pedziwiatr A T and Wielgosz R 2000 *J. Alloys Compounds* **307** 45
[35] Piquer C, Grandjean F, Long G J and Isnard O 2003 *J. Alloys Compounds* **353** 33
[36] Piquer C, Grandjean F, Isnard O, Pop V and Long G J 2004 *J. Alloys Compounds* **377** 1
[37] Paul-Boncour V, Wiesinger G, Reichl C, Latroche M, Percheron-Guégan A and Cortes R 2001 *Physica* B **307** 277
[38] Paul-Boncour V, Giorgetti C, Wiesinger G and Percheron-Guégan A 2003 *J. Alloys Compounds* **356/357** 195
[39] Gelato L 1981 *J. Appl. Crystallogr.* **14** 151
[40] Switendick A E 1979 *Z. Phys. Chem. N F* **117** 89
[41] Latroche M, Paul-Boncour V, Percheron-Guégan A and Bourée-Vigneron F 1997 *J. Solid State Chem.* **133** 568
[42] Hahn T (ed) 1987 *International Tables for Crystallography* vol A (Dordrecht: Reidel)
[43] Paul-Boncour V, Filipek S M, Marchuk I, André G, Bourée F, Wiesinger G and Percheron-Guégan A 2003 *J. Phys.: Condens. Matter* **15** 4349
[44] Paul-Boncour V, Guillot M, André G, Bourée F, Wiesinger G and Percheron-Guégan A 2005 *J. Alloys Compounds* at press
[45] Wagner F E and Wortmann G 1978 *Hydrogen in Metals I* vol 28, ed G Alefeld and J Völkl (Berlin: Springer) chapter 6 (Mössbauer Studies of Metal–Hydrogen Systems)
[46] Walker L R, Wertheim G K and Jaccarino V 1961 *Phys. Rev. Lett.* **6** 98
[47] Coehoorn C 1989 *Phys. Rev.* B **39** 13072
[48] Mohn P and Schwarz K 1985 *Physica* B+C **130** 26
[49] Matar S F and Paul-Boncour V 2000 *CR Acad. Sci. Paris* II **3** 27
[50] Oppelt A and Buschow K H J 1973 *J. Phys. F: Met. Phys.* **3** L212
[51] de Groot C H, de Boer F R, Buschow K H J, Hautot D, Long G J and Grandjean F 1996 *J. Alloys Compounds* **233** 1611
[52] Hautot D, Long G J, de Groot C H and Buschow K H J 1998 *J. Appl. Phys.* **83** 1554
[53] Paul-Boncour V and Matar S 2004 *Phys. Rev.* B **70** 184435 1
[54] Singh D J and Gupta M 2004 *Phys. Rev.* B **69** 132403
[55] Nakamura Y 1983 *J. Magn. Magn. Mater.* **31–34** 829
[56] Sakakibara T, Mitamura H and Goto T 1994 *Physica* B **201** 127
[57] Gignoux D and Schmitt D 1995 *Magnetic Properties of Intermetallic Compounds* (*Handbook of the Physics and Chemistry of Rare Earths* vol 20) ed K A Gschneidner Jr and L Eyring Jr (Amsterdam: Elsevier) p 293
[58] Fruchart D, Berthier Y, de Saxce T and Vulliet P 1987 *J. Solid State Chem.* **67** 197